

Shear-Induced Order in Suspensions of Hard Spheres

Bruce J. Ackerson^(a) and P. N. Pusey

Royal Signals and Radar Establishment, Malvern, Worcestershire WR14 3PS, United Kingdom

(Received 23 May 1988)

Suspensions in a liquid of "nearly hard" colloidal spheres were subjected to steady and oscillatory shear flows and studied by light scattering. Samples which exhibit a fluidlike ordering of the particles in equilibrium were induced to a solidlike order by oscillatory shear of strain amplitude ≈ 1 . In steady shear flow the suspensions showed evidence of "string" structures similar to but less complete than those found in computer simulations of simple liquids.

PACS numbers: 82.70.Dd, 05.40.+j, 05.70.Ln, 81.40.-z

In this Letter we describe studies by light scattering of some nonequilibrium structures of concentrated suspensions of colloidal spheres formed by the application of both oscillatory and steady shear flows. Probably our most interesting finding is that the application of a small-amplitude oscillatory shear, imposing a strain of order 1 on a suspension in which the equilibrium arrangement of particles is fluidlike, can cause strong particle ordering: Essentially an oscillating, three-dimensionally ordered colloidal crystal is formed. With increasing amplitude of applied oscillatory shear a range of structures, showing less pronounced order, is observed. Finally, with steady applied shear a weaker ordering remains. We compare the steady shear results with computer experiments on simple fluids and show also that the observed ordering of the particle structure is correlated with shear-thinning rheological behavior.

The particles used in these experiments consisted of polymethylmethacrylate (PMMA) cores stabilized sterically by a thin layer, ≈ 10 nm, of poly-(12-hydroxystearic acid).¹ Measurements by light scattering gave a particle diameter of $0.99 \mu\text{m}$ with a relative standard deviation less than 0.05. The particles were dispersed either in pure decalin or in a mixture of decalin and tetralin in proportion (3.06:1, by weight) chosen to nearly match the particle refractive index (≈ 1.51), thus providing nearly transparent samples with strong single scattering of light but relatively weak multiple scattering. The turbidity was $\approx 0.2 \text{ cm}^{-1}$ but could be reached further by adjustment of the solvent mixture. Rather the mixture was chosen to place the first minimum in the particle form factor at larger values of scattered wave vector than that of the first Debye-Scherrer ring. Multiple scattering does not influence the features described in this communication, these features being the same for the mixture and pure decalin solvents. Samples covering a range of concentration were prepared as described previously.¹ As in two earlier studies of similar but smaller particles,¹ we found the phase behavior with increasing particle volume fraction ϕ in the following sequence: colloidal fluid \rightarrow colloidal fluid + colloidal crystal \rightarrow fully colloidal crystal \rightarrow colloidal glass. As before we assume

the interparticle interaction to be close to "hard sphere" and identify the concentration at which crystallization is first observed with an effective hard-sphere volume fraction $\phi_E = 0.494$, the freezing concentration found in computer simulation of hard spheres.² Values of ϕ_E for the remaining samples were then calculated by appropriate scaling of their measured weight fractions, $\phi_E = 1.04\phi_W$.

Light-scattering measurements were made in a Couette shear cell with an inner radius of 10 mm and gaps between 0.25 and 1 mm, which are at least 250 times the particle diameter so that boundary-layer effects should be negligible. Indeed measurements made using the 1.00-mm gap were found to be in essential agreement with those obtained with smaller gaps. The available steady shear rates ranged from 0.002 s^{-1} to 200 s^{-1} ; observation of the translation of the speckle pattern formed by laser light scattered directly from the rotor verified the uniformity of motion at low rates.³ For scattering experiments the beam from a He-Cd laser (442 nm) was focused weakly and directed through the cell in the horizontal plane, normal to the vertical axis of rotation. The cell was immersed in a rectangular glass container filled with a liquid of refractive index ≈ 1.49 ; the scattering was observed on a paper screen attached to one wall of the bath. Although the sample, glass shear cell, and bath liquid were closely matched optically, some refraction of the light did occur and accounts for the slightly asymmetric scattering patterns observed in Figs. 1(d), 1(f), and 1(h). The incident beam could be translated across the width of the cell to probe different regions of reciprocal space, defined by the shear (\mathbf{K}_V), velocity (\mathbf{K}_V), and vorticity ($\mathbf{K}_e = \mathbf{K}_V \times \mathbf{K}_V$) directions [see Figs. 1(a) and 1(b)].

Figures 1(c) and 1(d) show the scattering from an equilibrated sample just below the freezing concentration ($\phi_E \sim 0.48$). A featureless Debye-Scherrer (DS) ring is observed, as expected for a dense fluidlike structure. The scattering by a single particle, the form factor, is determined by its core (shell) structure and shows a deep minimum at scattering vector just greater than that corresponding to the DS ring. Thus the intensity of the higher-order scattering, being the product of the form

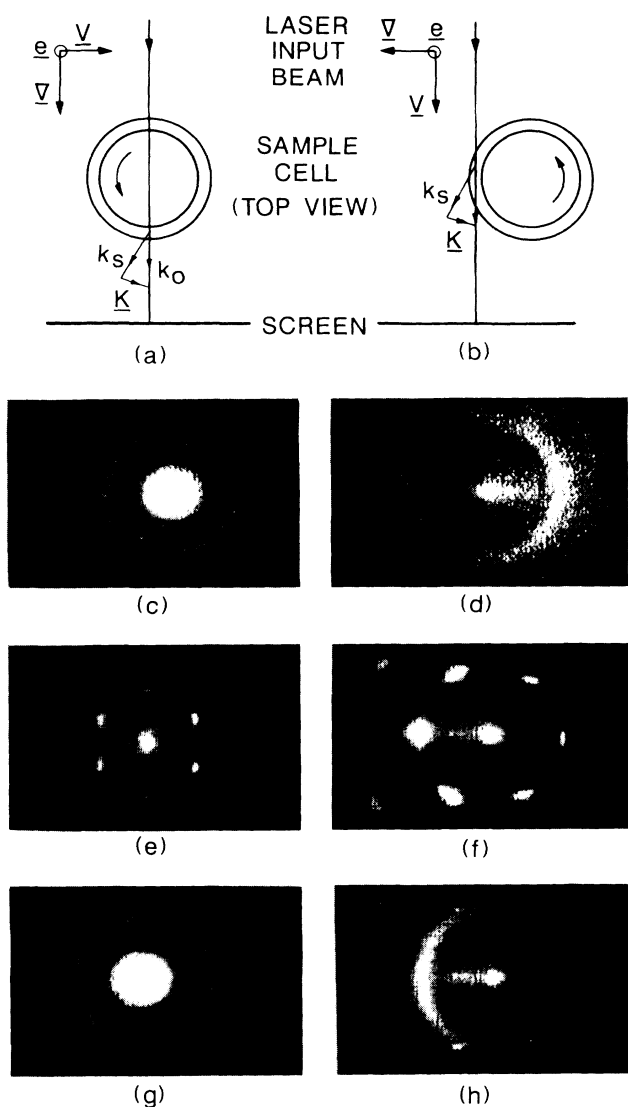


FIG. 1. (a), (b) Top view of shear cell showing orientation of the main scattering geometries: v is the velocity, V the shear, and e the vorticity. The scattering vector K is the difference between the incident k_0 and scattered k_s wave vectors. (c)–(h) Side views, as seen on screen, of scattering from a sample of $\phi_E \sim 0.48$: (c), (d), at equilibrium; (e), (f), oscillatory strain ≈ 4 ; (g), (h), steady shear flow $\sigma_R \sim 30$. Note weak intensity maxima in (h).

and structure factors, is weak and hard to observe.

An important measure of the relative effects on suspension structure and dynamics of an imposed shear flow and the natural Brownian motion of the particles is the reduced stress (or Péclet number) $\sigma_R = \dot{\gamma} \eta_E R^3 / k_B T$, where η_E is the shear viscosity of the suspension at shear rate $\dot{\gamma}$, R the particle radius, and $k_B T$ the thermal energy⁴. σ_R is the product of shear rate $\dot{\gamma}$ and a Brownian relaxation time $\tau = R^2 / (k_B T / \eta_E \dot{\gamma})$ (> 5 s for our samples). Significant distortion of an equilibrium structure is expected for $\sigma_R > 1$, where the influence of shear

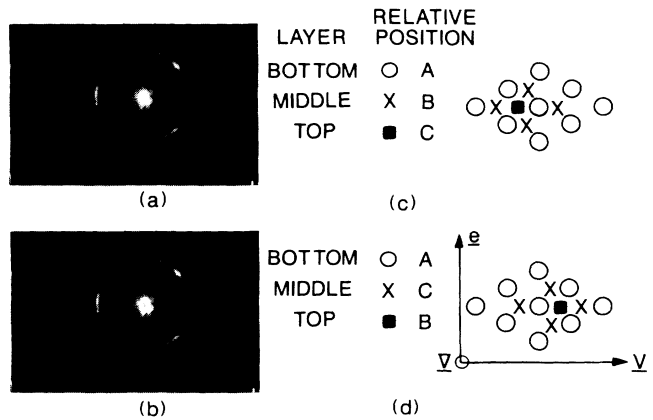


FIG. 2. Sample of $\phi_E \sim 0.48$ under oscillating strain ≈ 1.0 : (a), (b) scattering patterns observed on screen near extremes of oscillation cycle in configuration of Fig. 1(a); the exposure times of the photographs spanned about $\frac{1}{10}$ of the oscillation cycle. (c), (d) Depiction of the corresponding fcc crystal structures. Note the relatively easy transition between the two twin structures for this strain amplitude.

exceeds that of Brownian motion.⁵ We now describe the major features observed in light-scattering shear experiments for the $\phi_E = 0.48$ sample and present our interpretations.

For values of the applied oscillatory strain much less than unity, we observe a small distortion of the diffraction ring which follows the shear and decays rapidly when the shear is stopped. This is consistent with the expected behavior at small driving amplitudes.⁶ However, when the strain is of order unity, we see a redistribution of intensity within the diffraction ring which grows with time and some evidence of higher-order Bragg scattering. Figures 2(a) and 2(b) show the scattering in approximately the $K_V - K_e$ plane [i.e., in the scattering configuration of Fig. 1(a)] when the sample has been subjected to an oscillatory strain of about unity for about 30 min at a frequency of 1.0 Hz ($\sigma_R \sim 5$). Figure 2(a) is taken close to one extreme of the oscillation cycle and 2(b) close to the other. Thus the diffraction pattern oscillates between threefold symmetries with different orientations. Both qualitative considerations and computer calculations show these patterns to be consistent with the real-space structures sketched in Figs. 2(c) and 2(d). A face-centered-cubic structure, with one set of (111) planes parallel to the cell walls, oscillates between twins described by ... ABCA ... and ... ACBA ... stackings of hexagonally packed layers. The threefold reflections then arise from the changing orientations of the other three sets of (111) planes. We do not yet fully understand the extension of the Bragg reflections around the diffraction ring. It is possible that curvature of the cell plays a role, that the structure is really polycrystalline (or hexatic⁷), or that the strain amplitude is too large, resulting in a deforma-

tion of the perfect fcc structure. When the applied shear is stopped, the pattern of scattered light intensity reverts within about 30 min to the amorphous structure of Fig. 1(c), i.e., the crystal melts.

The detailed nature of the mechanism by which the system is driven into this structure is uncertain at present. Nevertheless we suspect that a minimum-energy dissipation principle may explain the structures observed.⁸ In an fcc crystal a particle can slide fairly freely over about one diameter in the "grooves" formed by the neighboring layers [see Figs. 2(c) and 2(d)]. This allows the crystal to strain or "flow" relatively easily for strains up to ≈ 1 . Furthermore, the hydrodynamic dissipation should be minimal as the particles maintain a relatively large average separation.

For strains of the fcc structure greater than ≈ 1 , more extensive motion of a particle in the same direction is "blocked" by particles in neighboring layers. As a result larger amplitude strains lead to a reorganization of the suspension order. Figures 1(e) and 1(f) show the scattering by a similar sample which has been subjected to a 1.0-Hz oscillatory strain of amplitude about 4. In the $K_V - K_e$ plane we now find a roughly hexagonal pattern of spots whose positions and intensities vary much less strongly during the oscillation cycle. As is apparent from comparison of Fig. 1(e) with Figs. 2(a) and 2(b), the hexagonal pattern found in the $K_V - K_e$ plane with strains greater than 1 is rotated by 30° with respect to the threefold patterns found with strains of order unity. In the $K_V - K_e$ plane, probed when the edge of the cell is illuminated [Fig. 1(b)], this structure gives a roughly hexagonal pattern with equatorial spots on the first ring [see Fig. 1(f)]. These two scattering patterns are consistent with a sliding layer structure⁹ having hexagonally close-packed layers parallel to the cell walls as for the fcc structure. However, the closest packed direction within a layer is now parallel to V , rather than e as in the fcc structure. A given particle in a layer must move past several neighbors in adjacent layers. The direction of easiest motion is a zig-zag path whose average direction is parallel to the mean flow velocity.

Several distinct structures related to these two major structures have been observed at other oscillatory strain amplitudes. Although we have not fully investigated all such structures, we make the following qualitative observation: As the amplitude is increased towards a quarter turn of the rotor (a strain of about 60) the order in the diffraction patterns is increasingly "washed out." However, in the $K_V - K_e$ plane there are still clear remnants of the diffraction spots observed at lower amplitudes. Not surprisingly similar results are found in the steady shear measurements, which we now describe.

When the equilibrated fluidlike sample is subjected to a steady shear flow, the scattering patterns [Figs. 1(c) and 1(d)] distort continuously with increasing shear to an elliptical form in a manner qualitatively similar to

that predicted by analytic theories^{10,11} and observed elsewhere.^{5,12} The maximum displacement dk of the DS ring saturates at $dk/k_{DS} \sim 0.1$, when the reduced stress (σ_R), defined above, reaches about 1. As $\dot{\gamma}$ is increased above the value, $\approx 0.2 \text{ s}^{-1}$, corresponding to $\sigma_R \sim 1$, distinct intensity maxima begin to develop in the $K_V - K_e$ plane [Fig. 1(h)]. While the amplitudes of these maxima increase with increasing $\dot{\gamma}$, they never completely replace the diffuse DS ring characteristic of the distorted fluidlike phase. Furthermore, no localized intensity maxima are observed in the $K_V - K_e$ plane [Fig. 1(g)] or in other scattering geometries.

Preliminary viscosity measurements on our samples are in reasonable agreement with recent work on similar systems.¹³ For concentrated samples, strong shear-thinning behavior was found: For $\phi_E \sim 0.48$, η_E decreased by a factor of about 8 between low and high $\dot{\gamma}$. A reduced stress, $\sigma_R \sim 1$, corresponded to shear rates well into the shear-thinning regime.

We now discuss and interpret these steady shear results in the light of other work. In qualitative agreement with our observations for $\sigma_R < 1$, described above, several analytic theories have predicted that the initial stages of shear thinning are associated with distortion of the fluidlike equilibrium structure.^{10,11,14} For higher shear rates, $\sigma_R > 1$, there appears to be no directly applicable theoretical work or computer simulation. The latter would require a nonequilibrium Brownian dynamics calculation which includes proper treatment of hydrodynamic interactions. However, a number of molecular-dynamics simulations of the effect of shear on atomic fluids have been reported¹⁵⁻¹⁹ and it has been suggested that these could apply, at least qualitatively, to particles in suspension.^{15,20} Many of these studies find that an imposed shear flow can, relatively early in the shear-thinning process, order the atoms (particles) into "strings" aligned parallel to the flow velocity. In some cases the strings form hexagonally ordered arrays in the $K_V - K_e$ plane. Our observation of distinct intensity maxima in the $K_V - K_e$ plane [Fig. 1(h)] is consistent with such an array having rows of strings in planes of constant velocity, i.e., parallel to the walls of the shear cell. However, the relative weakness of the effect in the $K_V - K_e$ plane and the absence of any significant structure in the diffraction patterns observed in other scattering geometries conflicts with the rather complete spatial ordering found at high shear rates in some of the molecular simulations.¹⁵⁻¹⁷

We offer several reasons why our suspension results might disagree with simulations on a relatively small number of atoms. (i) It is possible that pronounced stringlike order exists in our samples but that the hexagonal planes are not pinned to the vorticity direction except near the cell walls. This could cause smearing of the diffraction patterns in a manner similar to that observed. (ii) Molecular-dynamics simulations may not ap-

ply to suspensions. They do not take account of the liquid in which the particles are suspended either in terms of its intrinsic contribution to the suspension viscosity or in terms of the strong and complicated many-particle hydrodynamic interactions which might affect particle ordering at high rates of shear and high particle concentrations. Furthermore, it has recently been suggested that much of the order found in such simulations may be an artifact of an incorrect algorithm.²¹

In conclusion we note that the ability to produce solid-like order in an equilibrium fluid state by imposing an oscillatory shear is intriguing in itself; it may also have practical application, for example, in materials fabrication. Our steady shear measurements give some insight into the microscopic mechanisms underlying the technologically important rheological properties of suspensions, though much remains to be done. Elsewhere we will report similar measurements on suspensions at other concentrations, including samples whose equilibrium structures are crystalline and glassy and which show more pronounced order under steady shear.

One of us (B.J.A.) wishes to thank the personnel at the Royal Signals and Radar Establishment (RSRE) for their hospitality and help during his stay and to acknowledge the financial support of the RSRE, travel support by the International Program of the National Science Foundation Grant No. INT-8521429, and partial salary and communication support by the Low Temperature Physics Program of the National Science Foundation Grant No. DMR-8500704. We also thank R. H. Ottewill and D. M. Metcalfe for providing the particles, J. W. Goodwin for advice and the use of his rheometer, G. P. King for suggestions concerning the design of the shear cell, and L. Woodcock, S. Hess, D. Heyes, and P. M. Chaikin for valuable discussions.

^(a)Permanent address: Department of Physics, Oklahoma State University, Stillwater, Oklahoma 74078.

¹P. N. Pusey and W. van Meegen, *Nature (London)* **320**, 340 (1986), and *Phys. Rev. Lett.* **59**, 2083 (1987).

²W. G. Hoover and F. H. Ree, *J. Chem. Phys.* **49**, 3609 (1968).

³P. N. Pusey, *J. Phys. D* **9**, 111 (1976).

⁴I. M. Krieger, *Adv. Colloid Interface Sci.* **3**, 111 (1972).

⁵N. A. Clark and B. J. Ackerson, *Phys. Rev. Lett.* **44**, 1005 (1980). Note that for molecular liquids $\tau \sim 10^{-12}$ s so that unattainably high shear rates would be required to achieve $\sigma_R \sim 1$.

⁶H. N. W. Lekkerkerker, private communication.

⁷L. T. Shi and W. Krakow, *Phys. Rev. B* **34**, 7407 (1986).

⁸M. Doi, *J. Chem. Phys.* **59**, 5080 (1983).

⁹B. J. Ackerson and N. A. Clark, *Phys. Rev. Lett.* **46**, 123 (1981), and *Phys. Rev. A* **30**, 906 (1984).

¹⁰D. Ronis, *Phys. Rev. Lett.* **52**, 473 (1984), and *Phys. Rev. A* **29**, 1453 (1984), and **34**, 1472 (1986).

¹¹S. Hess, *Phys. Rev. A* **22**, 2844 (1980); J. F. Schwarzl and S. Hess, *Phys. Rev. A* **33**, 4277 (1986).

¹²B. J. Ackerson, J. van der Werff, and C. G. de Kruif, *Phys. Rev. A* **37**, 4819 (1988).

¹³W. J. Frith, Ph.D. Thesis, Katholieke Universiteit, Leuven, The Netherlands, 1986 (unpublished); see, however, G. N. Choi and I. M. Krieger, *J. Colloid Interface Sci.* **113**, 101 (1986).

¹⁴W. P. Russel and A. P. Gast, *J. Chem. Phys.* **84**, 1815 (1986).

¹⁵L. V. Woodcock, *Phys. Rev. Lett.* **54**, 1513 (1985).

¹⁶D. M. Heyes, *J. Chem. Soc. Faraday Trans. 2* **82**, 1365 (1986), and *Mol. Phys.* **57**, 1265 (1986).

¹⁷S. Hess, *Int. J. Thermophys.* **6**, 657 (1985).

¹⁸D. M. Heyes, G. P. Morriss, and D. J. Evans, *J. Chem. Phys.* **83**, 4760 (1985).

¹⁹J. J. Erpenbeck, *Phys. Rev. Lett.* **52**, 1333 (1984).

²⁰J. Rainwater, H. J. M. Hanley, N. A. Clark, and B. J. Ackerson, *J. Chem. Phys.* **79**, 4448 (1983).

²¹D. J. Evans and G. P. Morriss, *Phys. Rev. Lett.* **56**, 2172 (1986).

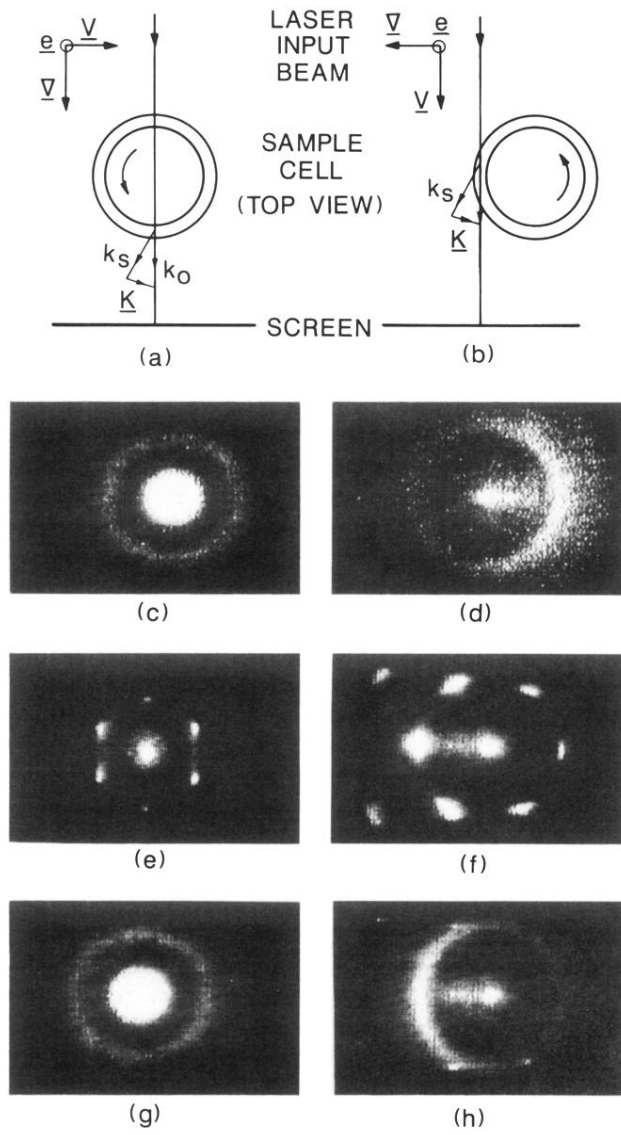


FIG. 1. (a),(b) Top view of shear cell showing orientation of the main scattering geometries: v is the velocity, ∇ the shear, and e the vorticity. The scattering vector K is the difference between the incident k_0 and scattered k_s wave vectors. (c)-(h) Side views, as seen on screen, of scattering from a sample of $\phi_E \sim 0.48$: (c),(d), at equilibrium; (e),(f), oscillatory strain ≈ 4 ; (g),(h), steady shear flow $\sigma_R \sim 30$. Note weak intensity maxima in (h).

